JPET Fast Forward. Published on April 15, 2015 as DOI: 10.1124/jpet.115.223107
This article has not been copyedited and formatted. The final version may differ from this version.

A novel partial agonist of PPARγ with excellent effect on insulin resistance and type 2 diabetes

Hui-juan Liu, Cheng-yu Zhang, Fei Song, Ting Xiao, Jing Meng, Qiang Zhang, Cai-li Liang, Shan Li, Jing Wang, Bo Zhang, Yan-rong Liu, Tao Sun and Hong-gang Zhou

Tianjin Key Laboratory of Molecular Drug Research, Tianjin International Joint Academy of Biomedicine, Tianjin, People's Republic of China (H.-j.L., C.-y.Z., F.S., T.X., J.M., Q.Z., C.-l.L., S.L., J.W., B.Z., Y.-r.L.).

The State Key Laboratory of Medicinal Chemical Biology, College of Pharmacy, Nankai University, Tianjin, People's Republic of China (T.S., H.-g.Z.).

Running title page

Running title: A novel partial agonist of PPARγ

Corresponding author

Dr. Hong-gang Zhou, The State Key Laboratory of Medicinal Chemical Biology, College of Pharmacy, Nankai University, Tianjin 300071, People's Republic of China, Email: hgzhou964@163.com, Tel.: +8613602042014.

The number of text pages: 31

The number of tables: 1

The number of figures: 9

The number of references: 32

The number of words in the abstract: 145

The number of words in the introduction: 432

The number of words in the discussion: 747

Abbreviations: PPARγ, peroxisome proliferator-activated receptor γ; TZDs, thiazolidinediones; DEX, dexamethasone; HepG2, human hepatocarcinoma cells; MDCK, Madin-Darby canine kidney; DMEM, dulbecco's minimum essential medium; FBS, fetal bovine serum; GOD-POD, glucose oxidase-peroxidase; MTT, 3-(4,5-dimethylthiazol-2-yl)-2,5-diphenyltetrazolium bromide; DMSO, dimethyl sulfoxide; MS, mass spectrometry, LBD, ligand-binding domain; OGTT, oral glucose tolerance test; LDH, lactate dehydrogenase; GS, glycogen synthase; GSK, glycogen synthase kinase; LC-MS, liquid chromatography-mass spectrometry; FSG, fasting serum glucose; TC, total cholesterol; TG, triglyceride; LDL-c, low-density lipoprotein

cholesterol; HDL-c, high-density lipoprotein cholesterol.

A recommended section assignment:

Drug Discovery and Translational Medicine

JPET Fast Forward. Published on April 15, 2015 as DOI: 10.1124/jpet.115.223107
This article has not been copyedited and formatted. The final version may differ from this version.

ABSTRACT:

Partial agonists of peroxisome proliferator-activated receptor-γ (PPARγ) reportedly reverse insulin resistance in patients with type 2 diabetes mellitus. In this work, a novel non-thiazolidinedione partial PPARγ ligand MDCCCL1636 was investigated. The compound displayed partial agonist activity in biochemical and cell-based transactivation assays, and reversed insulin resistance. MDCCCL1636 showed a potential anti-diabetic effect on an insulin-resistance model of HepG2 human hepatoma cells. High-fat diet-fed streptozotocin (HFD-STZ)-induced diabetic rats treated with MDCCCL1636 for 56 d displayed reduced fasting serum glucose and reversed dyslipidemia and pancreatic damage without significant weight gain. Furthermore, MDCCCL1636 had lower toxicity in vivo and in vitro than pioglitazone. MDCCCL1636 also potentiated glucose consumption and inhibited the impairment in insulin signaling targets, such as AKT, GSK3β and glycogen synthase, in HepG2 human hepatoma cells. Overall, our results suggest that MDCCCL1636 is a promising candidate for the prevention and treatment of type 2 diabetes mellitus.

JPET Fast Forward. Published on April 15, 2015 as DOI: 10.1124/jpet.115.223107
This article has not been copyedited and formatted. The final version may differ from this version.

1. **Introduction**

Peroxisome proliferator-activated receptor γ (PPARγ) is a ligand-dependent nuclear receptor that regulates gene expression associated with glucose homeostasis and insulin sensitization (Evans et al., 2004; Lehrke et al., 2005; McKenna et al., 2009). PPARγ is expressed in the liver, fat, and skeletal muscle. PPARγ gene deletion leads to insulin resistance and diet-induced obesity in mice, indicating that PPARγ plays a regulatory role in lipid and glucose homeostases and tissue inflammation.

PPARγ is a valid molecular target for metabolic syndrome and type 2 diabetes (Walczak et al., 2002; Waki et al., 2007). Several chemically diverse full agonists of PPARγ, such as thiazolidinediones (TZDs), have been used as insulin-sensitizing drugs in type 2 diabetes. “Partial” agonists have recently been developed to reduce the side effects (e.g., weight gain, risk of heart attack and edema) of TZDs (Berger et al., 2005). “Full” and “partial” PPARγ agonists are categorized by their transcriptional activities in the cell-based reporter assay (Reginato et al., 1998). Partial PPARγ agonists possess higher safety margins than full PPARγ agonists (Berger et al., 2005). Recent studies have exerted considerable efforts to design partial PPARγ agonists that retain their insulin-sensitizing efficacy without significant side effects.

Insulin resistance, which results from the defective utilization of metabolites in insulin-targeted tissues, is the major cause of type 2 diabetes and obesity (Leclercq et al., 2007). The insensitivity of the liver to the biological effects of insulin leads to a decrease in insulin-induced glucose transport, and hence, Human hepatocarcinoma cells (HepG2) are a good experimental system to investigate insulin resistance and the

JPET Fast Forward. Published on April 15, 2015 as DOI: 10.1124/jpet.115.223107
This article has not been copyedited and formatted. The final version may differ from this version.

metabolic disorder (Postic et al., 2004). Dexamethasone (DEX) induces insulin resistance (Niels et al., 2009) by accelerating hepatic glucose production and proteometabolism and suppressing peripheral glucose transport and utilization. In this work, an in vitro insulin resistance cell model was established to screen active compounds that can reverse the insulin resistance (Sangeetha et al., 2010).

We searched for novel PPARγ agonists in a library of structurally diverse organic compounds and identified a novel non-thiazolidinedione partial PPARγ ligand, N-(4-hydroxyphenethyl)-3-mercapto-2-methylpropanamide (Fig. 1A, also known as MDCCCL1636), This ligand was synthesized in our laboratory (Li NN et al., 2014) and its partial activation of PPARγ and effect on insulin resistance reversal were assessed in vitro. The cytotoxicity and the developmental toxicity in zebrafish embryos treated with MDCCCL1636 were evaluated and compared with those treated with pioglitazone. MDCCCL1636 effectively improved glucose tolerance and total plasma cholesterol level in high-fat diet-fed streptozotocin (HFD-STZ)-induced diabetic rats. We also investigated the major markers involved in insulin signaling, such as phosphatidylinositol 3-kinase (PI3K) signaling, to elucidate the mechanism by which MDCCCL1636 reverses insulin resistance.

JPET Fast Forward. Published on April 15, 2015 as DOI: 10.1124/jpet.115.223107
This article has not been copyedited and formatted. The final version may differ from this version.

2. Materials and methods

2.1 Cells and animals

human hepatocarcinoma HepG2, HEK-293T, HEK-293, NIH-3T3, and Madin-Darby canine kidney (MDCK) cells were obtained from KAIJI Company (Nanjing, China). These cells were maintained in dulbecco's minimum essential medium (DMEM)/high glucose with 10% fetal bovine serum (FBS) at 37 °C in a humidified 5% CO_2 environment.

AB strain zebrafish (*Danio rerio*) was obtained from Tianjin International Joint Academy of Biomedicine. Normoglycemic Wistar albino rats were obtained from Vital River Laboratory Animal Technology Co., Ltd (Beijing, China).

2.2 Antibodies and reagents

Antibodies to phosphoAkt (Ser^{473}), phosphoGSK-3β (Ser^{9}) and phospho glycogen synthase (Ser^{645}) were purchased from Affinity (USA).

3-(4,5-dimethylthiazol-2-yl)-2,5-diphenyltetrazolium bromide (MTT) and dimethyl sulfoxide (DMSO) were purchased from Sangon Biotech (Shanghai, China). Glucose assay kit was purchased from Leadman Group Co. Ltd. (Beijing, China). STZ was purchased from Dalian Meilun Biotech Co., Ltd.

2.3 Methods

2.3.1 Transcriptional transactivation assay

HEK-293T cells cotransfected with pGal4-DBD (pBIND)-PPARγ-ligand-binding domain (LBD) fusion and pG5luc vector were used to measure the transcriptional transactivation activities of the compounds through luciferase reporter

JPET Fast Forward. Published on April 15, 2015 as DOI: 10.1124/jpet.115.223107
This article has not been copyedited and formatted. The final version may differ from this version.

assay (Elke et al., 2006). Approximately 204-505 residues of the human PPARγ-LBD were cloned into the pBIND to generate fusion proteins with the DNA-binding domain of GAL4. HEK-293T cells were grown in DMEM with 10% FBS at 37°C in 5% CO_2. HEK-293T cells were seeded in 96-well plates at a concentration of 2×10^4 cells per well. Lipofectamine 2000 transfection reagent was used for transfection. The recombinant plasmid pBIND-LBD (0.05 μg/well) and pG5luc vector (0.15 μg/well) were cotransfected into HEK-293T cells for 6 h. Subsequently, the cells were treated with various concentrations of MDCCCL1636 or pioglitazone for 24 h. The firefly luciferase activity was measured by using the ONE-GloTM Luciferase Assay System (Promega) in accordance with the manufacturer's protocol.

2.3.2 Mass spectrometry (MS) assay

The purified PPARγ-LBD protein [13] (methods for expression and purification of PPARγ-LBD are available in the supplementary materials) was diluted to 50 μM in 10 mM ammonium acetate and incubated with MDCCCL1636 in a 1:3 molar excess for 15 min. The PPARγ-LBD-MDCCCL1636 complex was analyzed with a Waters SYNAPT G1 High-Definition Mass Spectrometry.

2.3.3 Development of insulin-resistant model by using HepG2 cells

HepG2 cells were seeded in 96-well plates at a concentration of 1×10^4 cells per well and then treated in serum-free DMEM/high glucose overnight. Subsequently, the cells were induced with 100 nM, 1 μM, 5 μM, and 10 μM DEX for 24, 48, and 72 h. At selected time points, the cells were washed thrice with PBS and stimulated for 24 h with 1 nM insulin. Glucose uptake was detected by using a glucose assay kit. The kit

was used to detect the glucose level in the medium via the glucose oxidase-peroxidase (GOD-POD) method. Subsequently, we calculated the consumption of glucose. The best time point for the insulin-resistant model was determined by measuring the maximum inhibition in glucose uptake (Yuan et al., 2003)**.** The insulin-resistant model was validated using pioglitazone. The HepG2 cells were induced with 100 nM DEX for 24 h and then treated with varying concentrations of pioglitazone for 24 h with 1 nM insulin. Glucose uptake was detected by using a glucose assay kit.

2.3.4 Effect of MDCCCL1636 on glucose uptake in insulin-resistant HepG2 cells

MDCCCL1636 and pioglitazone were used to treat the normal control cells and insulin-resistant cells for 24 h to assess the effect of MDCCCL1636 and pioglitazone on glucose uptake. A glucose assay kit was used for the glucose uptake experiments.

2.3.5 Cytotoxicity assessment

MDCCCL1636 and pioglitazone were assessed for their cytotoxic effects on HEK-293, HepG2, NIH-3T3 and MDCK cells by using an MTT reagent. The assay was performed 24 h after treatment with varying concentrations of MDCCCL1636 and pioglitazone. Formazan concentration, which is directly proportional to cell viability, was measured at 492 nm.

2.3.6 Developmental toxicity assay in zebrafish embryos

AB line zebrafish was maintained in accordance with the standard procedures (M. Westerfield, 1994). The night before breeding, adult male and female zebrafish were placed in a breeding tank and then separated from each other with a mesh screen. The embryos were generated through natural mating the next morning, after turning on the

light and withdrawing the mesh screen. The embryos were collected within 30 min after spawning, rinsed thrice, transferred into Petri dishes containing the embryo medium, and then cultured at 28.5 °C.

The protocol described by Mark *et al.* (2004) was adopted in this experiment. The normal embryos were selected and transferred into a multiwell microplate with one embryo per well in 300 μL treatment solution. A total of 30 embryos at 4 h postfertilization were treated with various concentrations of MDCCCL1636 and pioglitazone, and the control group was treated with 0.1% DMSO. Developmental phenotypes were observed every 24 h for 96 h. All experiments were repeated thrice. The mortality and malformation rate of embryos were calculated at the end of the experiment. The study was performed in accordance with the national and institutional guidelines for animal welfare.

2.3.7 In vivo efficacy of MDCCCL1636 in HFD-STZ-induced type 2 diabetic rats

Normoglycemic male Wistar albino rats weighing 180–200 g were used. All rats, except for those in the normal control group, were fed with HFD (20% glucose, 10% egg yolk powder, 10% lard, 0.2% bile salts, 1.5% cholesterol, and 58.3% normal commercial pellet diet). After 10 d of HFD, the rats were fasted overnight for 12h and then given a single injection of freshly prepared solution of STZ (40 mg/kg) in citrate-phosphate buffer (0.1 M, pH 4.2) (Ashok et al., 2011). Hyperglycemia in the rats was assessed by measuring fasting serum glucose (FSG) levels, after 72 h of STZ administration. Rats with an FSG levels higher than 13.89 mmol/L were selected for the subsequent experiments (Ashok et al., 2011). The rats were randomly divided into

six groups of six animals each: (1) normal control group (rats without any treatment); (2) diabetic control group (diabetic rats treated with vehicle); (3) positive control group (diabetic rats treated with pioglitazone at 30 mg/kg/day); (4) high dose group of MDCCCL1636 (diabetic rats treated with MDCCCL1636 at 15 mg/kg/day); (5) medium dose group of MDCCCL1636 (diabetic rats treated with MDCCCL1636 at 7.5 mg/kg/day); (6) lower dose group of MDCCCL1636 (diabetic rats treated with MDCCCL1636 at 3.75 mg/kg/day). The treatment was continued for 56 days.

In the oral glucose tolerance test (OGTT) assay, 12 h fasted rats were administered with vehicle or drugs after FSG measurement, and then with an oral bolus of glucose (2 g/kg). Subsequently, the blood glucose level was measured at 0, 0.5, 1, and 2 h.

On the last day, FSG levels were measured and then blood was withdrawn from the heart. Serum was analyzed for triglyceride (TG), total cholesterol (TC), high-density lipoprotein cholesterol (HDL-c), and low-density lipoprotein cholesterol (LDL-c) after being separated by centrifugation at 3000 × *g* for 10 min. The animals were sacrificed, and the pancreas was subjected to histopathological studies (Kamalakkannan et al. 2004). The lipid profiles were assessed using commercial kits. Formalin-fixed pancreatic tissue was cut in 4μm thick sections and then stained with hematoxylin and eosin (H&E) (Ashok et al., 2011). The stained sections were blindly examined using a light microscope (Nikon, Tokyo, Japan). The study was performed in accordance with the national and institutional guidelines for animal welfare.

2.3.8 Effect of MDCCCL1636 on the expression of insulin signaling markers in

JPET Fast Forward. Published on April 15, 2015 as DOI: 10.1124/jpet.115.223107
This article has not been copyedited and formatted. The final version may differ from this version.

PI3K signaling

Insulin-sensitive cells, non-treated insulin-resistant cells, and MDCCCL1636 or pioglitazone-treated insulin-resistant cells were lysed at 4°C with RIPA lysis buffer. The cell lysates were subjected to SDS-PAGE and then Western blot analysis using anti-phospho antibodies for AKT, GSK3β, and GS.

2.3.9 Statistical analysis.

Datas were reported as mean ± SD. All data were analyzed using one-way analysis of variance (ANOVA) followed by Bonferroni post-hoc test (SPSS software package version 17.0). Statistical significance was considered at $p < 0.05$.

3 Results

3.1 Identification of the partial PPARγ agonist MDCCCL1636

MDCCCL1636 (Molecular Weight: 239.1 Da) was identified as a lead hit among a class of partial PPARγ ligands throgh transcriptional transactivation assay of a PPARγ agonist library. In HEK-293T cells, MDCCCL1636 (EC_{50} = 7.092 μM) was a partial agonist with 40% efficacy compared with pioglitazone (EC_{50} = 3.36 μM) at 100 μM (Fig. 1B).

3.2 Verifying the interaction of MDCCCL1636 and PPARγ-LBD

MS data revealed peaks corresponding to the molecular weight of the protein PPARγ-LBD and the complex PPARγ-LBD-MDCCCL1636. The molecular weights of the PPARγ-LBD protein the complex were 32910 Da (Fig. 2A) and 33146 Da (Fig. 2B), respectively. The difference in molecular weight between PPARγ-LBD protein and the PPARγ-LBD-MDCCCL1636 complex was 236 Da, which was approximately equal to the molecular weight of MDCCCL1636. This result demonstrated that the MDCCCL1636 strongly interacted with the ligand binding domain of human PPARγ.

3.3 Effect of MDCCCL1636 on the insulin-resistant model of HepG2 cells

3.3.1 Time and concentration course analyses of DEX induction on HepG2 cells

Time and concentration course analyses of DEX treatment at 100 nM, 1 μM, 5 μM, and 10 μM concentrations in 24, 48, and 72 h were performed. Insulin resistance of DEX was also assessed based on the inhibition of glucose uptake. Insulin-stimulated glucose uptake was reduced maximally to approximately 26.83% at 24 h of 100 nM DEX treatment compared with the control (Fig. 3A). Thus, treatment

JPET Fast Forward. Published on April 15, 2015 as DOI: 10.1124/jpet.115.223107
This article has not been copyedited and formatted. The final version may differ from this version.

with 100 nM DEX for 24 h was the optimal conditions for the establishment of insulin-resistant model.

Cell viability was assayed at different time points (24, 48, and 72 h) of DEX induction to eliminate the influence of DEX toxicity on the inhibition of glucose uptake. DEX exhibited no significant cytotoxicity to the cells at 24 h, which confirmed the insulin-resistant inducing effect of DEX on HepG2 cells (Fig. 3B).

3.3.2 Validation of DEX-induced insulin-resistant model

Pioglitazone was used as a positive control to determine the validity and the reversal properties of the DEX-induced insulin-resistant model. The induced HepG2 cells were treated with varying concentrations of pioglitazone for 24 h. Glucose uptake analysis showed that pioglitazone reversed the DEX-induced insulin resistance in a dose-dependent manner (Fig. 3C).

3.3.3 Glucose uptake potential of MDCCCL1636 on the DEX-induced insulin-resistant model

The effects of MDCCCL1636 and piogliltazone on insulin resistance were assessed and compared using the DEX-induced insulin-resistant model. MDCCCL1636 effectively restored the DEX-induced glucose uptake inhibition in a dose-dependent manner (Fig. 3D). MDCCCL1636 maximally augmented glucose uptake to approximately 45.13% at 150 μM in the DEX-induced insulin-resistant model. The response of MDCCCL1636 at 75 μM (approximately 41.45%) to insulin resistance reversal was higher than that of pioglitazone (34.82%).

3.4 Cytotoxicity of MDCCCL1636 and pioglitazone on HEK-293, HepG2,

NIH-3T3, and MDCK cells

The cytotoxic effects of MDCCCL1636 and pioglitazone on HEK-293, HepG2, NIH-3T3, and MDCK cells were assessed via a cytotoxicity assay. MDCCCL1636 showed negligible effect on cell viability, whereas pioglitazone exhibited about 25% (Figs. 4A-C) and 50% (Fig. 4D) toxic effects at its highest concentration. This result confirmed that MDCCCL1636 had lower cytotoxicity than pioglitazone.

3.5 Toxic effects of MDCCCL1636 and pioglitazone on embryonic development of zebrafish

The mortality rate of zebrafish embryos treated with various concentrations of MDCCCL1636 and pioglitazone for 96 h is presented in Fig. 5A. Treatment with 1 mM of pioglitazone for 96 h resulted in 95% embryo death compared with 65% embryo death after MDCCCL1636 treatment. MDCCCL1636 and pioglitazone showed dose-dependent lethal effects. The lethal concentration of MDCCCL1636 that caused 50% mortality (LC_{50}) in embryos was 742.569 μM, whereas that of pioglitazone was 390.226 μM. Exposure experiments revealed that the effective concentrations of MDCCCL1636 and pioglitazone to induce 50% malformations (EC_{50}) of the embryos was 916.044 μM and 420.741 μM (Fig.5B), respectively.

Pericardial edema and axial malformation were observed in embryos exposed to 50 mM pioglitazone, whereas no obvious malformation was observed in embryos exposed to less than 250 mM MDCCCL1636. Embryos only subjected to more than 500 mM MDCCCL1636, would showed pericardial edema, and those exposed to more than 750 mM MDCCCL1636 would have axial malformations (Fig. 6). These

results indicated that MDCCCL1636 exerted lower toxicity on zebrafish embryos than pioglitazone.

3.6 Hypoglycemic effect of MDCCCL1636 on HFD-STZ-induced type 2 diabetic rats

Administration of MDCCCL1636 at 15 mg/kg/day and pioglitazone at 30 mg/kg/day for 56 d resulted in a significant decrease in FSG compared with the diabetic control rats with a reduction of 20.72% and 18.73%, respectively.

As shown in Table 1, the HFD-STZ-induced diabetic rats had higher serum TG, TC, and LDL-c and significantly lower HDL-c than the normal control rats. Treatment with 7.5 mg/kg MDCCCL1636 and 30 mg/kg pioglitazone significantly reduced serum TG (53.5% and 31.7%, respectively) and TC (56.86% and 43.4%, respectively) compared with diabetic control rats. In addition, the rats treated with MDCCCL1636 and pioglitazone had significantly lower LDL-c (65.4% and 45.6%, respectively, $p<0.001$) while significantly higher HDL-c (16.1% and 9.7%, respectively) than the diabetic controls. Administration of pioglitazone at 30 mg/kg for 56 d resulted in a significant increase in body weight (12.13%), whereas MDCCCL1636-treated groups did not show significant changes in body weight in comparison with the diabetic control rats.

OGTT was performed in HFD-STZ-induced type 2 diabetic rats on day 42 of the treatment period. Afetr being challenged with an oral bolus of glucose, the MDCCCL1636-treated animals showed lower glucose excursion compared with the vehicle-treated diabetic animals. The results indicated that MDCCCL1636 improved

the impaired glucose tolerance of type 2 diabetic rats (Fig. 7).

Fig. 8A showed the histopathological changes in the pancreatic islet of the experimental groups..The number and area of islets in the pancreas (Figs. 8B-C) were also analyzed. Neither β-cell damage nor inflammatory changes were observed in the normal architecture of pancreatic islet (Fig. 8A1) . However, the β-cells were obviously damaged and the area of pancreatic islets was significantly reduced in the HFD-STZ induced diabetic rats (Fig. 8A2). Damage to the pancreatic islets and β-cell in the diabetic rats was restored by MDCCCL1636 and pioglitazone, as evidenced by their protective effects on β-cell damage (Figs. 8A3-4). Compared with pioglitazone, MDCCCL1636 also more effectively improved the fatty degeneration of renal tubular epithelial cells of the diabetic rats (supporting data are provided in the supplementary materials).

3.7 Effect of MDCCCL1636 and pioglitazone on insulin signaling in insulin-resistant cells

AKT Ser^{473} phosphorylation was reduced in insulin-resistant cells compared with control cells. The insulin-resistant cells showed 73.9% lower AKT Ser^{473} phosphorylation than control cells. Both pioglitazone and MDCCCL1636 significantly increased AKT Ser^{473} phosphorylation by approximately 1.86-fold and 3.68-fold, respectively, (Fig. 9A). AKT expression was similar in the normal control and insulin resistant cells. Both pioglitazone and MDCCCL1636 increased AKT Ser^{473} phosphorylation, although MDCCCL1636 showed better effects than pioglitazone.

JPET Fast Forward. Published on April 15, 2015 as DOI: 10.1124/jpet.115.223107
This article has not been copyedited and formatted. The final version may differ from this version.

GSK-3β Ser^{9} phosphorylation in the insulin-resistant cells was reduced by approximately 19.1% compared with that in the normal control cells. Pioglitazone and MDCCCL1636 increased GSK-3β phosphorylation in the insulin-resistant cells (Fig. 9B). GSK-3β expression was similar in the normal control and insulin-resistant cells. MDCCCL1636 and pioglitazone upregulated GSK-3β Ser^{9} phosphorylation by 0.53-fold and 0.21-fold, respectively.

Glycogen synthase Ser^{645} phosphorylation was higher in the insulin-resistant cells than in the normal control cells. DEX-treated insulin-resistant cells showed lower activity than the insulin-sensitive cells. Pioglitazone and MDCCCL1636 increased glycogen synthase activity by 62% and 70%, respectively, in the insulin-resistant cells compared with the normal control cells (Fig. 9C). GS expression was similar in the normal control and the insulin resistant cells. The insulin-resistant cells treated with MDCCCL1636 had higher GS activity than those treated with pioglitazone.

JPET Fast Forward. Published on April 15, 2015 as DOI: 10.1124/jpet.115.223107
This article has not been copyedited and formatted. The final version may differ from this version.

4. Discussion

This study introduced the partial PPARγ activator MDCCCL1636. Transactivation assay data confirmed that the propanamide derivative functions as a partial PPARγ agonist that strongly combines with PPARγ-LBD, as determined by MS.

Insulin-sensitizing agents could function as drugs to treat various metabolic disorders caused by insulin resistance (Kahn et al., 2000). An in vitro model that mimics insulin resistance was established to screen insulin-sensitive agents (Olivares-Reyes et al., 2009; Sakoda et al., 2000). The model mimicked the exact in vivo clinical insulin-resistant conditions, and it can be reversed by insulin-sensitizing drug treatment (Sakoda et al., 2000). In this work, a model of HepG2 cells was developed using DEX and the model was used to assess the potential of MDCCCL1636 in insulin resistance reversal. The extent of insulin resistance of the model was measured through the inhibition of glucose uptake. In this work, the maximum desensitization (approximately 26.83%) of insulin-stimulated glucose uptake was achieved after 24 h of 0.1 μM DEX treatment.

In this study, the TZDs pioglitazone was used to validate the developed resistance model. TZDs as insulin-sensitizing drugs reportedly reverse DEX-induced insulin resistance by suppressing the adverse effects of DEX on insulin sensitivity and glucose tolerance (Samuel, 2011; Willi et al., 2002). Concentration course analysis of the effect of pioglitazone on the insulin-resistant model revealed that TZD reversed DEX-induced insulin resistance in a dose-dependent manner. This study determined

whether or not MDCCCL1636 could also reverse the DEX-induced impairment in glucose uptake. Similar to pioglitazone, MDCCCL1636 showed potential reversal of DEX-induced insulin resistance as evidenced by the restoration of glucose uptake. MDCCCL1636 and pioglitazone showed similar effects on insulin resistance, however, MDCCCL1636 had lower toxicity on cells and zebrafish embryos than pioglitazone. This result may be ascribed to the partial PPARγ agonist activity of MDCCCL1636.

Rats fed with HFD may develop insulin resistance (Kraegen et al., 1991). In addition, low-dose STZ leads to a mild β cell dysfunction and impairment of insulin secretion, which result in hyperglycemia (Mythili et al., 2004). Thus, feeding rats with HFD and treating them with low-dose STZ (40 mg/kg) can mimic type II diabetes (Reed et al., 2000; Parveen et al., 2010). In the present work, the HFD-STZ-treated type 2 diabetic rats showed significantly increased serum glucose and β-cell dysfunction, as well as decreased body weight and dyslipidemia. Our results showd that MDCCCL1636 reduced the serum glucose level and improved the imparired glucose tolerance in type 2 diabetes.

In the HFD-STZ-induced diabetic rats, dyslipidemia was manifested in the increased levels of LDL-c, TG, and TC, and in reduced HDL-c levels. The hypercholesterolemia and hypertriglyceridemia observed in the model resulted from the increased absorption of TGs and TC from the HFD and from the elevated concentrations of very-low-density lipoproteins, which consequently increased LDL-c and reduced HDL-c levels (Zammit et al., 2001; Taskinen et al., 2003). In the present

JPET Fast Forward. Published on April 15, 2015 as DOI: 10.1124/jpet.115.223107
This article has not been copyedited and formatted. The final version may differ from this version.

work, MDCCCL1636 treatment significantly reduced the TG, TC, and LDL-c levels while increased the HDL-c level in the HFD-STZ-induced diabetic rats. MDCCCL1636 improves dyslipidemia possibly by inhibiting hepatic TG secretion or increasing peripheral TG clearance (Kamalakkannan et al., 2005). MDCCCL1636 reverses the insulin resistance, which consequently improves the lipid metabolism.

In the present study, MDCCCL1636 upregulated PI3K signaling. Our data suggested that DEX induced HepG2 cells insulin resistance by impairing the phosphorylation of insulin signaling proteins of AKT, GSK-3β, or GS. DEX treatment reduced insulin-stimulated AKT and GSK-3β phosphorylation and blocked the dephosphorylation and activation of GS.

In this study, DEX treatment reduced insulin-stimulated AKT Ser^{473} phosphorylation by approximately 73.9%. Both MDCCCL1636 and pioglitazone increased AKT Ser^{473} phosphorylation in the insulin-resistant cells, but the effect of MDCCCL1636 was 0.64-fold higher than that of pioglitazone. The insulin-resistant cells also exhibited 19.1% lower GSK-3β Ser^{9} phosphorylation than the normal control cells. MDCCCL1636 can reverse such a reduction. DEX inhibited the glycogen synthase activity. MDCCCL1636 and pioglitazone reduced GS phosphorylation by 70% and 62%, respectively. DEX induction significantly desensitized HepG2 cells toward insulin-stimulated glucose uptake (Pereira et al., 2008). The possibility of this desensitization can also be attributed to impairment in the insulin signaling targets, including AKT, GSK3β, and GS. Our results showed that MDCCCL1636 effectively restored DEX-induced desensitization by restoring AKT

and GSK3β phosphorylation and GS activity.

In conclusion, the novel compound MDCCCL1636 can partially activate PPARγ. MDCCCL1636 can also reduce FSG and reverse the dyslipidemia and damage of the pancreas without significantly increasing body weight. Moreover, MDCCCL1636 was less toxic in vivo and in vitro than pioglitazone. Therefore, MDCCCL1636 is a potential treatment for type 2 diabetes.

Authorship Contributions

Participated in research design: Sun, and Zhou;

Conducted experiments: Song, H.-j.Liu, C.-y.Zhang, Xiao, Meng, Liang, and Q. Zhang;

Performed data analysis: Song, H.-j.Liu, C.-y.Zhang, Li and Wang;

Wrote or contributed to the writing of the manuscript: Song, H.-j.Liu, C.-y.Zhang, B.Zhang, and Y.-r.Liu.

References

Sharma AK, Bharti S (2011) Upregulation of PPARγ by Aegle marmelos Ameliorates Insulin Resistance and β-cell Dysfunction in High Fat Diet Fed-Streptozotocin Induced Type 2 Diabetic Rats. Phytother. Res.25: 1457–1465.

Berger JP, Akiyama TE, Meinke PT (2005) PPARs: therapeutic targets for metabolic disease. Trends Pharmacol Sci 26: 244–251.

Burgermeister E, Schnoebelen A, Flament A, Benz J, Stihle M, Gsell B, et al. (2006) A Novel Partial Agonist of Peroxisome ProliferatorActivated Receptor-γ (PPARγ) Recruits PPARγ-Coactivator-1γ, Prevents Triglyceride Accumulation, and Potentiates Insulin Signalingin Vitro. Molecular Endocrinology 20(4): 809–830.

Evans RM, Barish GD, Wang YX (2004) PPARs and the complex journey to obesity. Nat Med 10: 355–36.

Huang JT, Welch JS, Ricote M, Binder CJ, Willson TM, Kelly C, et al. (1999) Interleukin-4-dependent production of PPAR-γ ligands in macrophages by 12/15-lipoxygenase. Nature 400: 378–382.

Kahn BB, Flier JS (2000) Obesity and insulin resistance. Journal of Clinical Investigation 106: 473–481.

Kamalakkannan N, Prince P SM (2004) Antidiabetic and antioxidant activity of Aegle marmelosextract in streptozotocin induced diabetic rats. Pharm Bio l42: 125–130.

Kamalakkannan N, Prince P SM (2005) Antihyperlipidemic effect of Aegle marmelosfruit extract in streptozotocin induced diabetic in rats. J Sci Food Agric 85:

569–573.

Kraegen EW, Clark PW, Jenkins AB, Daley EA, Chisholm DJ, Storlien LH (1991) Development of muscle insulin resistance after liver insulin resistance in high-fat-fed rats. Diabetes 40:1397–1403.

Lehrke M, Lazar MA (2005) The many faces of PPARγ. Cell 123: 993–999.

Leclercq IA, Morais ADS, Schroyen B, van Hul N, Geerts A (2007) Insulin, resistance in hepatocytes and sinusoidal liver cells: mechanisms and consequences. Journal of Hepatology 47: 142–156.

Li NN, Xu YT, Xian Q, Bai CG, Wang TY, Wang L, et al. (2014) Simplified captopril analogues as NDM-1 inhibitors, Bioorg. Med. Chem. Lett., 24: 386–389.

Reimers MJ, Flockton AR, Tanguay RL (2004). Ethanol- and acetaldehyde-mediated developmental toxicity in zebrafish. Neurotoxicology and Teratology 26: 769–781.

McKenna NJ, Cooney AJ, DeMayo FJ, Downes M, Glass CK, Lanz RB, et al (2009) Minireview: evolution of NURSA, the Nuclear Receptor Signaling Atlas. Mol Endocrinol 26: 740–746.

Mythili MD, Vyas R, Akila G, Gunasekaran S (2004) Effect of streptozotocin on the ultrastructure of rat pancreatic islets. Microsc Res Tech 63: 274–281.

M. Westerfield (1994) The Zebrafish Book: A Guide to the Laboratory Use of the Zebrafish (Brachydanio rerio), University of Oregon Press, Eugene, OR.

Moller N,, Jorgensen JOL (2009) Effects of growth hormone on glucose, lipid, and protein metabolism in human subjects. Endocr Rev 30(2): 152–177.

Olivares-Reyes JA, Arellano-Plancarte A, Castillo-Hernandez JR (2009) Angiotensin II and the development of insulin resistance: implications for diabetes. Molecular and Cellular Endocrinology 302: 128–139.

Parveen K, Khan MR, Mujeeb M, Siddiqui WA (2010) Protective effects of pycnogenol on hyperglycemia-induced oxidative damage in the liver of type 2 diabetic rats. Chem Biol Interact 186: 219–227.

Postic C, Dentin R, Girard J (2004) Role of the liver in the control of carbohydrate and lipid homeostasis. Diabetes and Metabolism 30: 398–408.

Pereira S, Marliss EB, Morais JA, Chevalier S, Gougeon R (2008) Insulin Resistance of Protein Metabolism in Type 2 Diabetes. Diabetes 57(1): 56-63.

Reed MJ, Meszaros K, Entes LJ et al. (2000) A new rat model of type 2 diabetes: the fat-fed, streptozotocin-treated rat. Metabolism 49: 1390–1394.

Reginato MJ, Bailey ST, Krakow SL, Minami C, Ishii S, Tanaka H, et al. (1998) A potent antidiabetic thiazolidinedione with unique peroxisome proliferator-activated receptor γ-activating properties. J Biol Chem 27332679–32684.

Sakoda H, Ogihara T, Anai M, Funaki M, Inukai K, Katagiri H, et al. (2000) Dexamethasone-induced insulin resistance in 3T3-L1 adipocytes is due to inhibition of glucose transport rather than insulin signal transduction. Diabetes 49: 1700–1708.

Samuel, VT (2011) Fructose induced lipogenesis: from sugar to fat to insulin resistance. Trends in Endocrinology and Metabolism 22: 60–65.

Sangeetha KN, Sujatha S, Muthusamy VS, Anand S, Nithya N, Velmurugan D, et al. (2010) 3β-Taraxerol of Mangifera indica, a PI3Kinase dependent dual activator of

glucose transport and glycogen synthesis in 3T3-L1 adipocytes. Biochimica et Biophysica Acta 1800(3) 359–366.

Taskinen MR (2003). Diabetic dyslipidaemia: from basic research to clinical practice. Diabetologia 46: 733–749.

Waki H, Park KW, Mitro N, Pei L, Damoiseaux R, Wilpitz DC, et al. (2007) The small molecule harmine is an antidiabetic cell-type-specific regulator of PPARγ expression. Cell Metab 5: 357–370.

Walczak R, Tontonoz P (2002) PPARadigms and PPARadoxes: expanding roles for PPARγ the control of lipid metabolism. J Lipid Res 43: 177–186.

Willi SM, Kennedy A, Wallace P, Ganaway E, Rogers NL, Garvey WT (2002) Troglitazone antagonizes metabolic effects of glucocorticoids in humans: effects on glucose tolerance, insulin sensitivity, suppression of free fatty acids, and leptin. Diabetes 51: 2895–2902.

Yuan L, Ziegler R, Hamann A (2003) Metformin modulates insulin-postreceptor signalling transduction in chronically insulin treated HepG2 cells. Acta Pharmacologica Sinic 24(1): 55.

Zammit VA, Waterman IJ, Topping D, McKay G (2001) Insulin stimulation of hepatic triacylglycerol secretion and the etiology of insulin resistance. J Nutr131: 2074–2077.

Footnotes

This study was supported by the National Natural Science Funds of China (81102374, 81201650), the key technologies R & D program of Tianjin (14ZCZDSY00038).

Hui-juan Liu, Cheng-yu Zhang, and Fei Song contributed equally to this study.

JPET Fast Forward. Published on April 15, 2015 as DOI: 10.1124/jpet.115.223107
This article has not been copyedited and formatted. The final version may differ from this version.

Figure Legends

Fig. 1. (A) Structure of N-(4-hydroxyphenethyl)-3-mercapto-2-methylpropanamide. (B) Representative concentration–response curves of reporter gene transactivation by MDCCCL1636 compared with pioglitazone. Stand and error bars represent three independent experiments, and each experiment was performed in triplicate. All values are expressed as mean ± SD. Significance level was determined by one-way ANOVA followed by Bonferroni post-hoc test. $^{\#\#}p < 0.05$, $^{\#\#\#}p < 0.001$ vs. normal control.

Fig. 2. (A) Mass spectra of PPARγ-LBD protein, (B) PPARγ-LBD-MDCCCL1636 complex.

Fig. 3. Insulin-resistant cell model and drug screening. (A) Time and concentration course analyses of DEX induction in HepG2 cells. (B) Effect of DEX induction on cytotoxicity. (C) Validation of DEX-induced insulin-resistant model. (D) Comparative assessment of glucose uptake potential of MDCCCL1636 and pioglitazone on the insulin-resistant model of HepG2 cells. Stand and error bars represent three independent experiments and each experiment was conducted in triplicate. $^{**}p < 0.05$ and $^{***}p < 0.01$ vs. insulin resistance control; $^{\#\#}p < 0.05$, $^{\#\#\#}p < 0.001$ vs. normal control.

Fig. 4. Cytotoxicity of MDCCCL1636 and pioglitazone. Cytotoxicity of MDCCCL1636 and pioglitazone on (A) HEK-293, (B) HepG2, (C) NIH-3T3, and (D) MDCK cells. Stand and error bars represent three independent experiments, and each experiment was performed in triplicate.

Fig. 5. Cytotoxicity of MDCCCL1636 and pioglitazone on the embryonic

development of zebrafish. (A) Lethality curve of embryos exposed to MDCCCL1636 or pioglitazone. The LC_{50} of MDCCCL1636 and pioglitazone were 742.569 μM (r^2=0.993) and 390.226 μM (r^2=0.985), respectively. (B) Malformation curve of embryos exposed to MDCCCL1636 or pioglitazone. The EC_{50} of MDCCCL1636 and pioglitazone were 916.044 μM (r^2=0.971) and 420.741 μM (r^2=0.999), respectively.

Fig. 6. Concentration-dependent developmental toxicity endpoints in zebrafish.

Embryos were exposed to either water or to the indicated MDCCCL1636 or pioglitazone concentrations. Lateral view of 96 hpf embryos revealing numerous malformations. Axial malformation, AM; pericardial edema, PE.

Fig. 7. Effect of MDCCCL1636 and pioglitazone on oral glucose tolerance in normal and HFD-STZ induced diabetic rats. (A) Blood glucose curves in the oral glucose tolerance test. (B) Area under the curve in the oral glucose tolerance test. All values are expressed as mean ± SD. Significance was determined by one-way ANOVA followed by Bonferroni post-hoc test, $^{**}p < 0.01$ vs. diabetic control.

Fig. 8. Histopathological changes in the pancreatic islets of rats in the experimental groups. (A1) Light micrograph of normal control rats showing normal β-cells in the pancreatic islet (H & E, 200×), (A2) HFD-STZ-induced diabetic control rats showing pancreatic islet damage (H&E, 200×), (A3) MDCCCL1636 at 7.5 mg/kg/day reversed pancreatic islet damage (H&E, 200×), (A4) pioglitazone at 30 mg/kg/day reversed pancreatic islet damage (H&E, 200×). (B) Islets number analysis of experimental groups. (C) Islets area analysis of experimental groups. All values are expressed as mean ± SD. Significance was determined by one-way ANOVA followed by

Bonferroni post-hoc test, $^{**}p < 0.01$ vs. normal control.

Fig. 9. Effect of MDCCCL1636 and pioglitazone on insulin signaling in insulin-resistant cells. HepG2 cells were incubated with or without 100 nM DEX for 24 h and in 1 nM insulin with or without the drugs (pioglitazone or MDCCCL1636) for another 24 h. Cell lysates were separated by SDS-PAGE and subjected to Western blot analysis with (A) anti-phosphoAkt (ser473) antibody, (B) anti-phosphoGSK-3β (Ser^{9}) antibody, and (C) anti-phospho glycogen synthase (Ser^{645}) antibody. Data are expressed as a percentage of the normal control. $^{**}p < 0.05$, $^{***}p < 0.001$ vs. insulin resistance control; $^{\#\#}p < 0.05$, $^{\#\#\#}p < 0.001$ vs. normal control.

Table 1. Effects of MDCCCL1636 on body weight and biochemical parameters of normal and diabetic rats. All values are expressed as mean ± SD. Significance level was determined by one-way ANOVA followed by Bonferroni post-hoc test. [a]$p < 0.001$ vs. normal control; [b]$p < 0.05$, [c]$p < 0.001$ vs. diabetic control.

Biochemical parameter	Normal Control	Diabetic Control	Pioglitazone	MDCCCL1636		
			30 mg/kg	3.75 mg/kg	7.5 mg/kg	15 mg/kg
FSG (mmol/L)	5.6±0.9	25.1±2.9[a]	20.4±2.8[c]	21.8±2.3[b]	20.9±1.9[c]	19.9±1.1[c]
TG (mmol/L)	0.81±0.10	1.01±0.27[a]	0.69±0.19[c]	0.74±0.26[b]	0.47±0.15[c]	0.42±0.12[c]
TC (mmol/L)	1.47±0.18	8.88±3.64[a]	5.03±1.27[b]	4.80±0.76[b]	3.83±1.11[c]	4.40±0.78[c]
HDL-C (mmol/L)	0.78±0.01	0.62±0.12[a]	0.68±0.13[b]	0.67±0.13[b]	0.72±0.07[c]	0.77±0.10[c]
LDL-C (mmol/L)	0.26±0.03	2.98±1.44[a]	1.62±1.27[b]	1.46±0.56[c]	1.03±0.49[c]	1.21±0.70[c]
Body Weight (g)	553.85±22.71	365.09±12.53[a]	409.37±16.39[b]	379.94±22.46	376.27±21.24	380.51±7.49

JPET Fast Forward. Published on April 15, 2015 as DOI: 10.1124/jpet.115.223107
This article has not been copyedited and formatted. The final version may differ from this version.

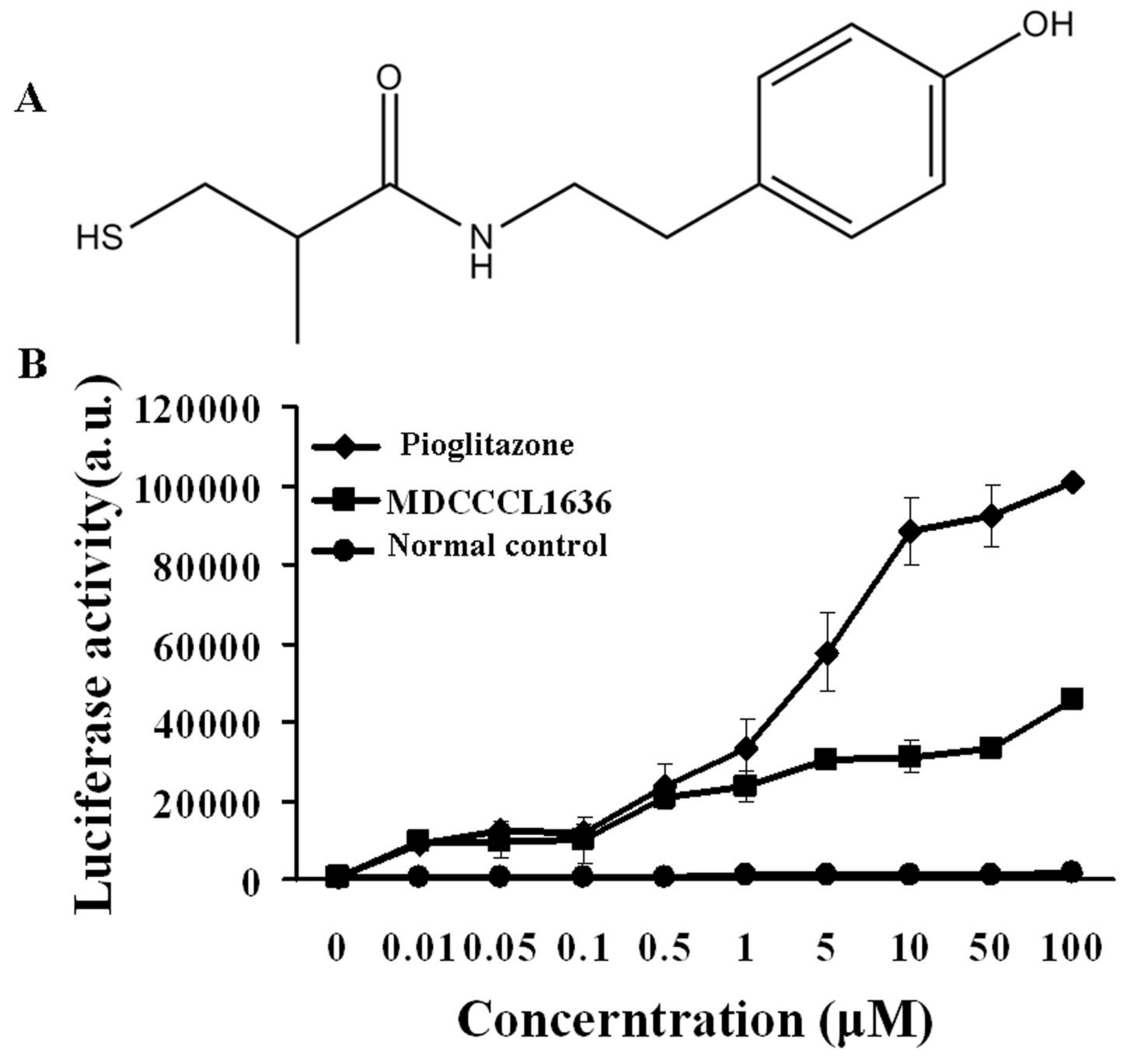
A
OH
O
HS
N
H
B
Luciferase activity(a.u.)
120000
100000
80000
60000
40000
20000
0
Pioglitazone
MDCCCL1636
Normal control
0
0.01
0.05
0.1
0.5
1
5
10
50
100
Concerntration (μM)

Fig.1

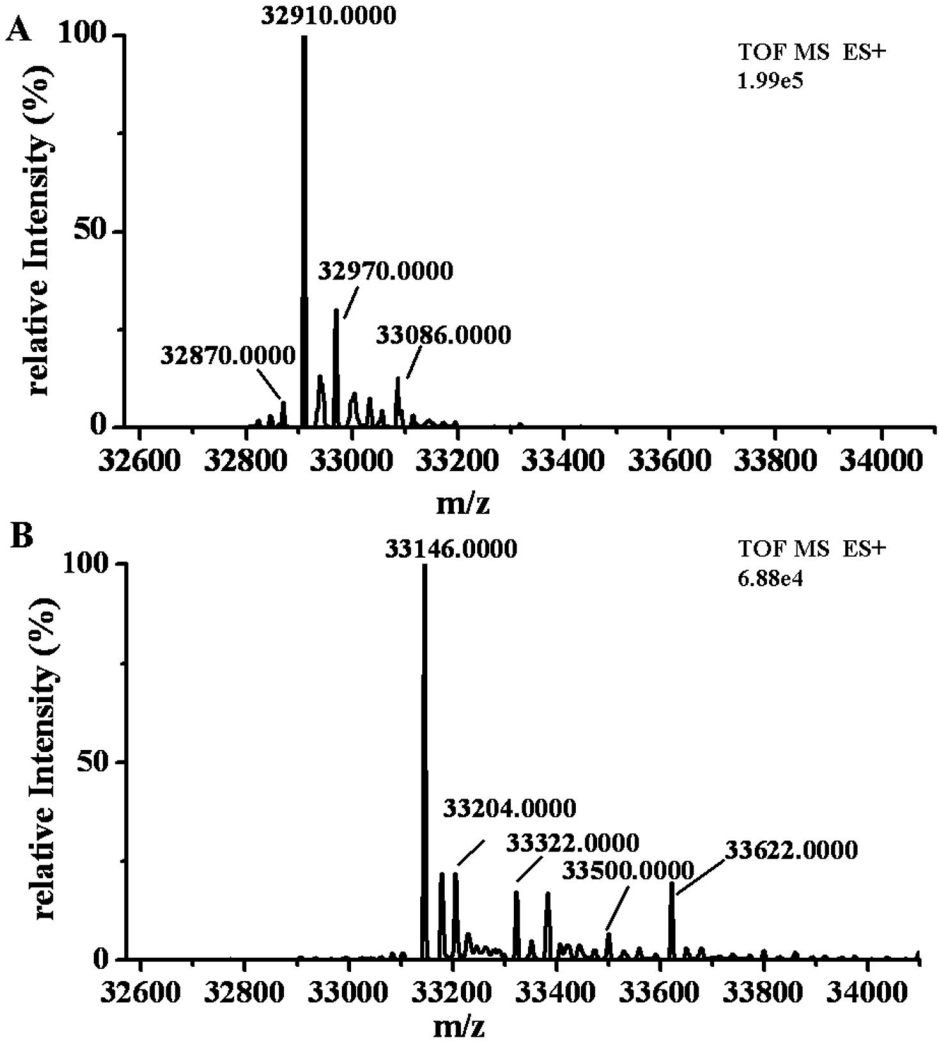
A
100
50
0
relative Intensity (%)
32910.0000
32970.0000
33086.0000
32870.0000
TOF MS ES+
1.99e5
32600 32800 33000 33200 33400 33600 33800 34000
m/z
B
100
50
0
relative Intensity (%)
33146.0000
33204.0000
33322.0000
33500.0000
33622.0000
TOF MS ES+
6.88e4
32600 32800 33000 33200 33400 33600 33800 34000
m/z

Fig. 2

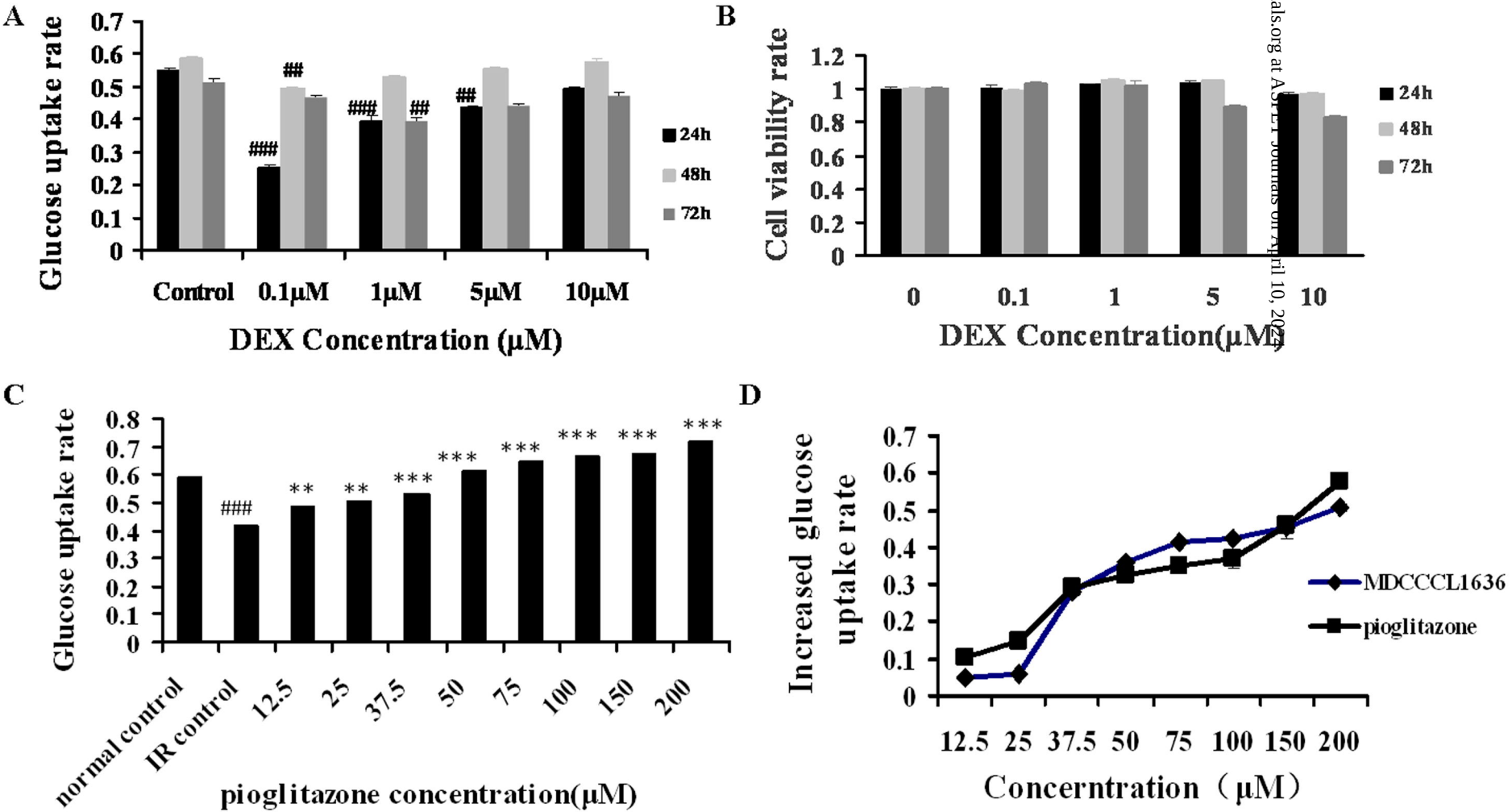

Fig. 3

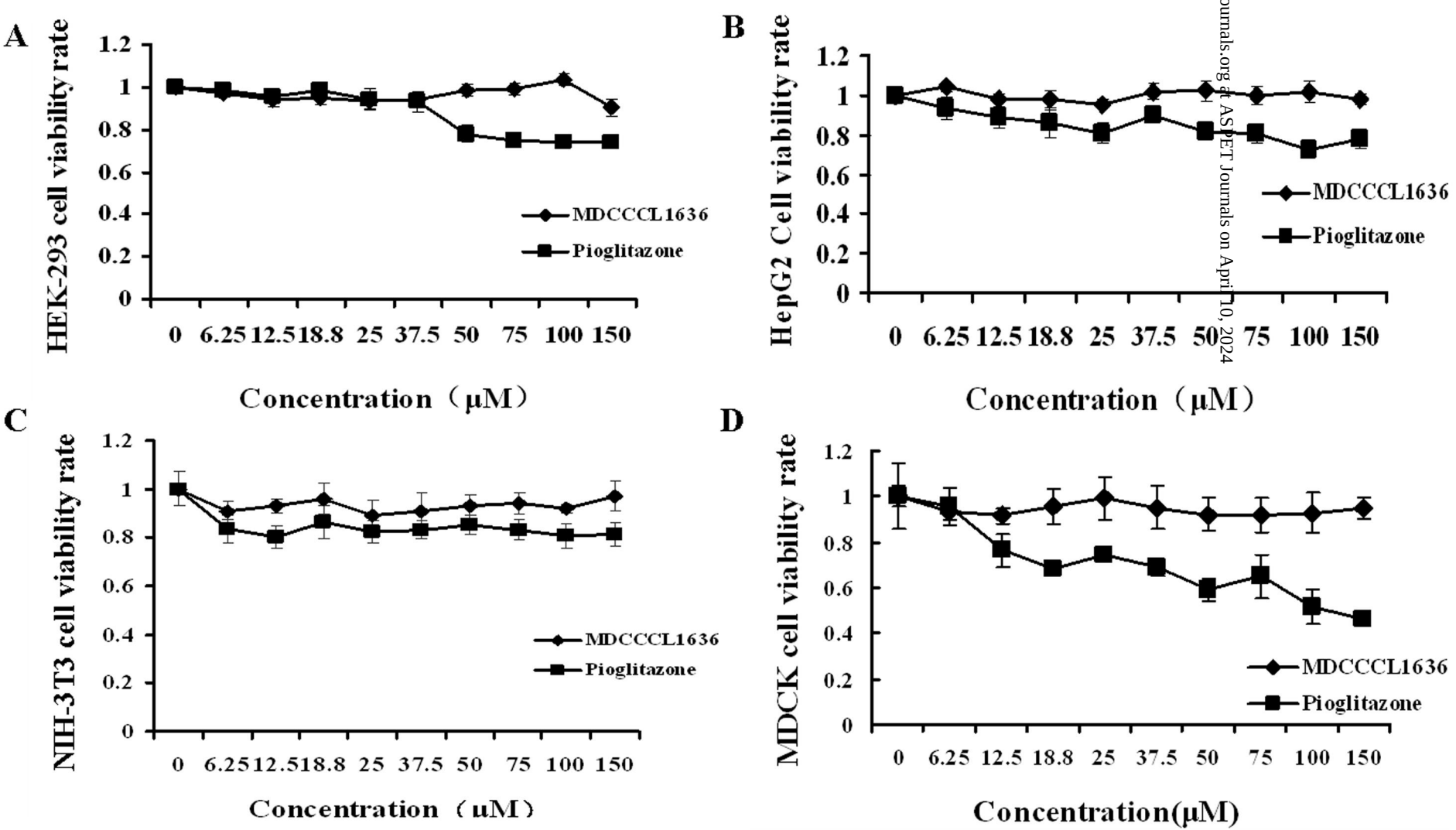

Fig. 4

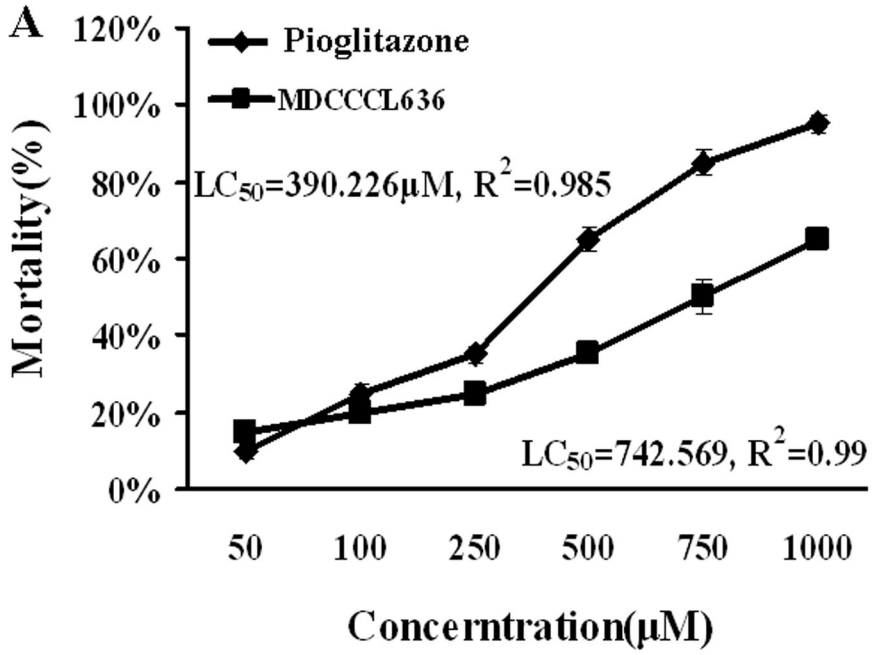

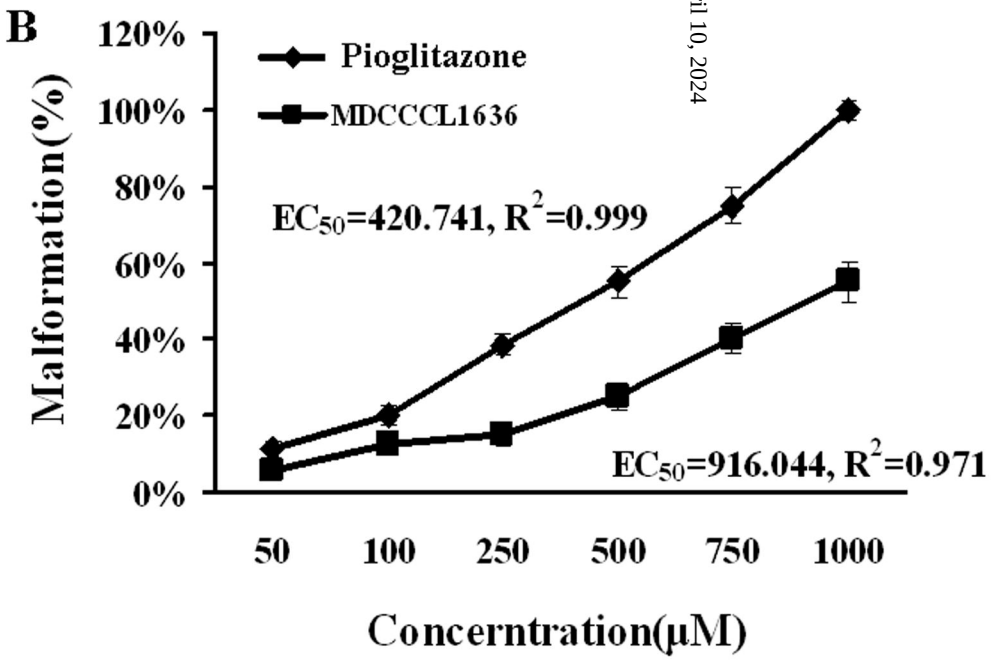

Fig.5

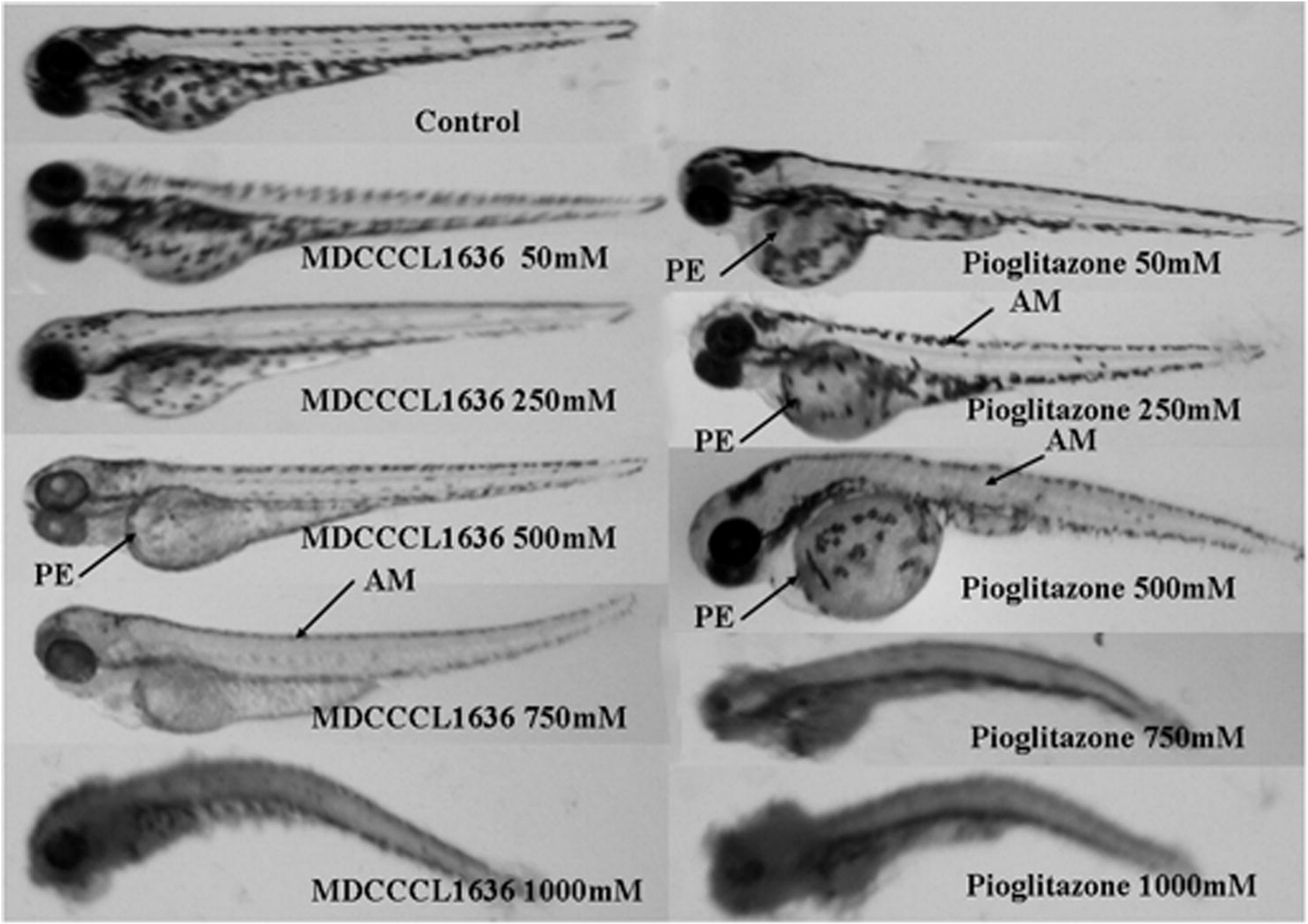
Control
MDCCCL1636 50mM
MDCCCL1636 250mM
MDCCCL1636 500mM
PE
AM
MDCCCL1636 750mM
MDCCCL1636 1000mM
PE
Pioglitazone 50mM
AM
PE
Pioglitazone 250mM
AM
PE
Pioglitazone 500mM
Pioglitazone 750mM
Pioglitazone 1000mM

Fig. 6

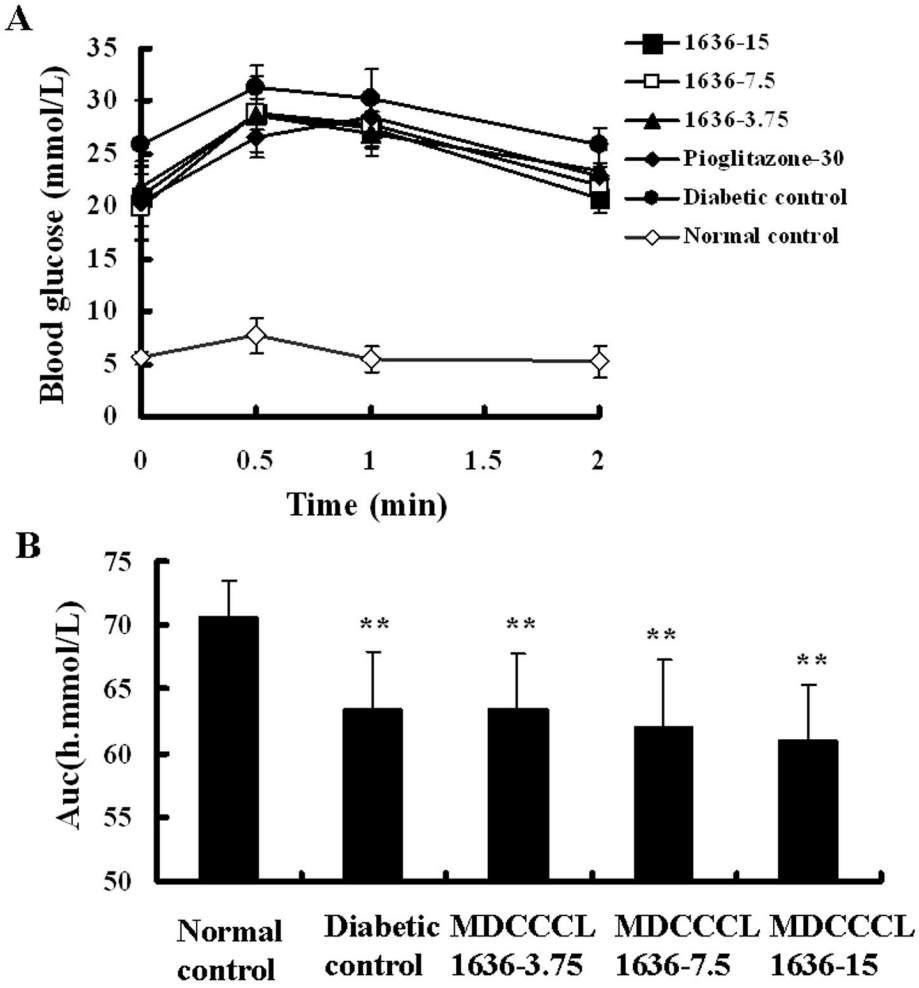
A
Blood glucose (mmol/L)
35
30
25
20
15
10
5
0
0
0.5
1
1.5
2
Time (min)
1636-15
1636-7.5
1636-3.75
Pioglitazone-30
Diabetic control
Normal control
B
Auc(h.mmol/L)
75
70
65
60
55
50
**
**
**
**
Normal control
Diabetic control
MDCCCL 1636-3.75
MDCCCL 1636-7.5
MDCCCL 1636-15

Fig. 7

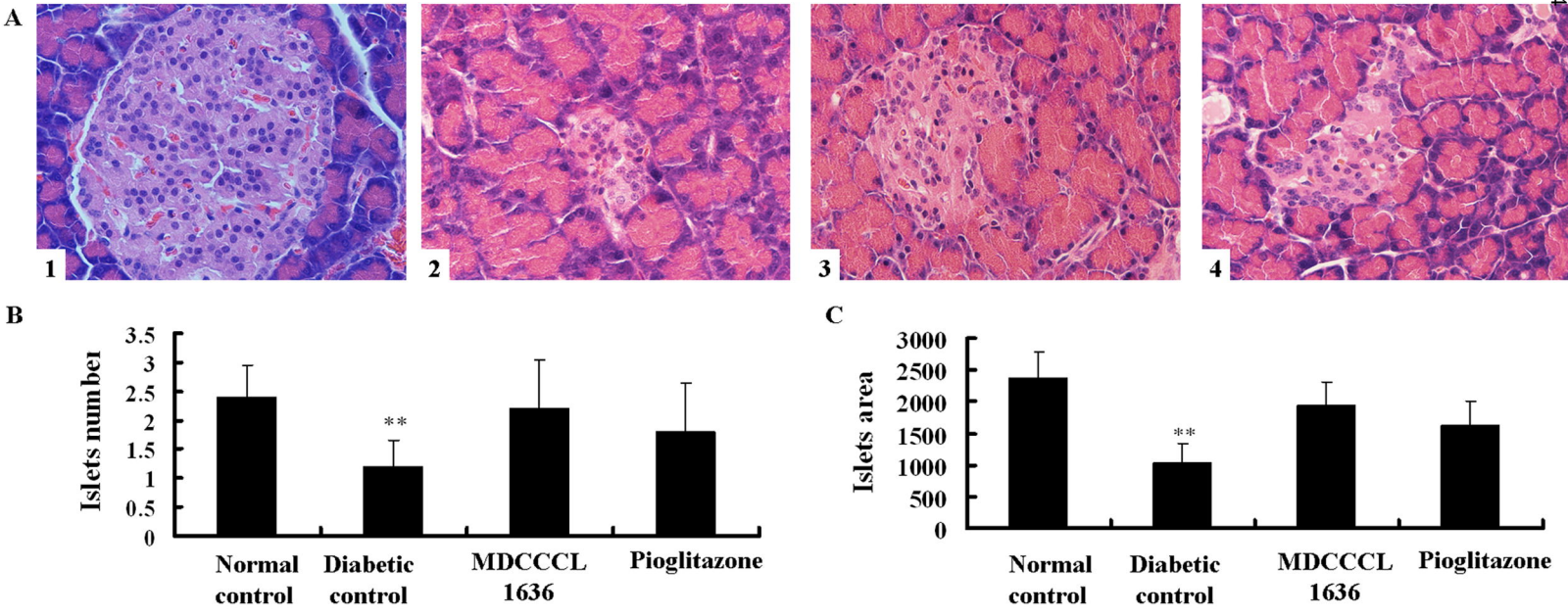
A
1
2
3
4
B
Islets number
3.5
3
2.5
2
1.5
1
0.5
0
**
Normal control
Diabetic control
MDCCCL 1636
Pioglitazone
C
Islets area
3000
2500
2000
1500
1000
500
0
**
Normal control
Diabetic control
MDCCCL 1636
Pioglitazone

Fig. 8

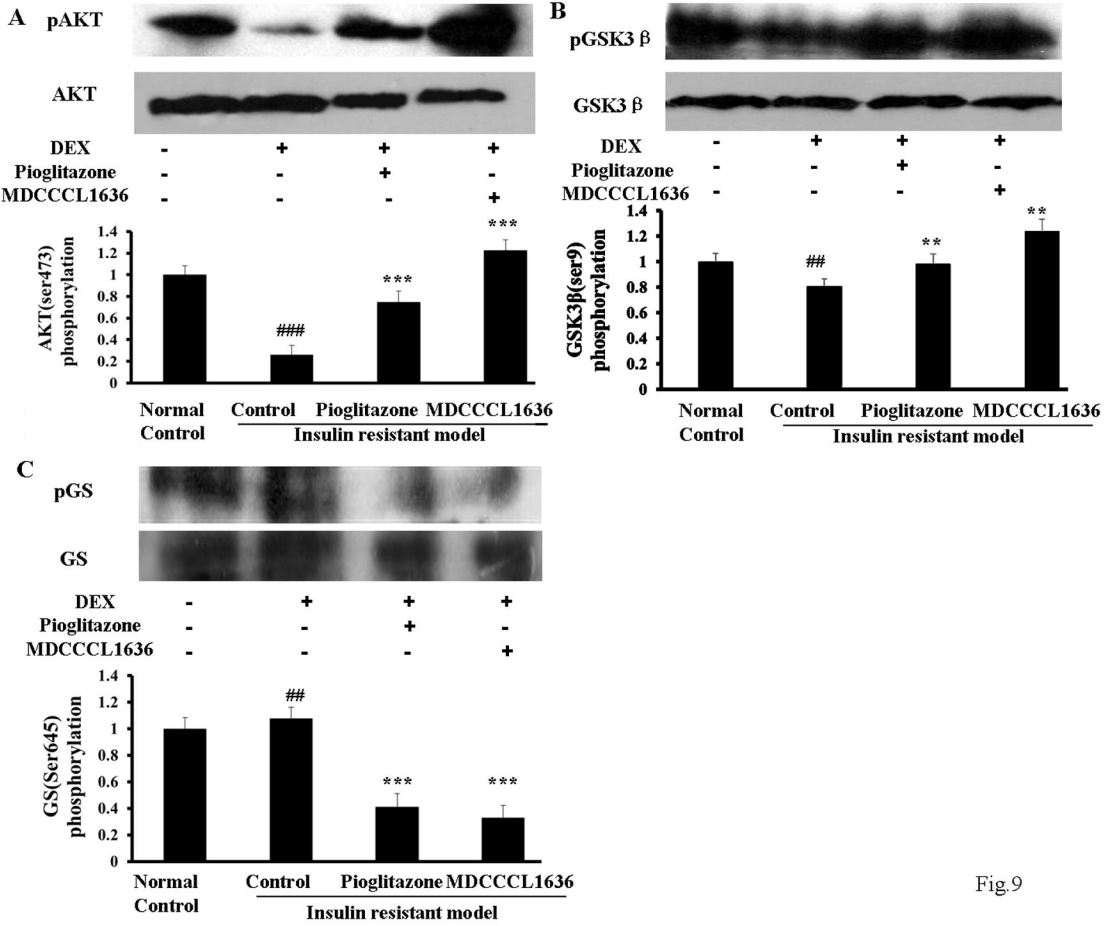
A
pAKT
AKT
DEX
Pioglitazone
MDCCCL1636
AKT(ser473) phosphorylation
###
***
Normal Control
Control
Pioglitazone
MDCCCL1636
Insulin resistant model
B
pGSK3 β
GSK3 β
GSK3β(ser9) phosphorylation
##
**
C
pGS
GS
GS(Ser645) phosphorylation

Fig.9

A novel partial agonist of PPARγ with excellent effect on insulin resistance and type 2 diabetes

Hui-juan Liu, Cheng-yu Zhang, Fei Song, Ting Xiao, Jing Meng, Qiang Zhang, Cai-li Liang, Shan Li, Jing Wang, Bo Zhang, Yan-rong Liu, Tao Sun and Hong-gang Zhou

1. Methods for expression and purification of PPARγ-LBD

The PPARγ-LBD (the ligand binding domain of human PPARγ, residues 206–477) was cloned into the expression vector pET15b. *E.coli* BL21 (DE3) host cells transformed with this expression plasmid were grown in LB at 37 °C to an A_{600} of 1 and induced with 0.1 mM IPTG at 16 °C [13]. The cells were harvested, resuspended in extract buffer (50 mM Tris, pH 8.0, 250 mM NaCl, and 10% glycerol), and lysed by French press. The lysate was centrifuged at 12,000 rpm for 30 min. The supernatant was loaded onto a Ni-affinity column. The column was washed with extract buffer, and the protein was eluted with wash buffer (50 mM Tris, pH 8.0, 250 mM NaCl, 10% glycerol, and 100 mM imidazole). The protein was further purified on a Superdex 200 column.

Fig. S1

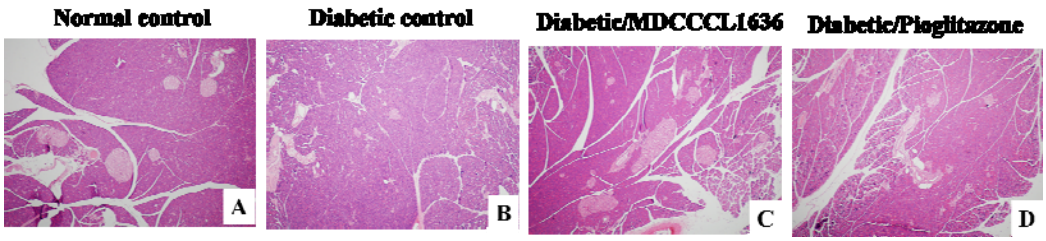

Fig.S2

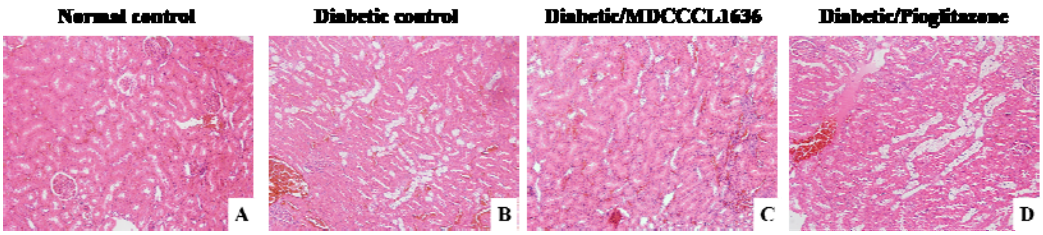

Figure legends:

Fig. S1. Histopathological changes in islets of pancreas of experimental groups. (A) Light micrograph of normal control rats showing normal β -cells in pancreatic islet (H & E, 40x), (B) HFD-STZ induced diabetic control rats showing pancreatic islet damage (H & E, 40x), (C) MDCCCL1636 at 7.5 mg/kg/day resulted in the reversal of pancreatic islet damage (H & E, 40x), (D) pioglitazone at 30 mg/kg/day resulted in the reversal of pancreatic islet damage (H & E, 40x).

Fig. S2. Histopathological changes in renal tubular epithelial cells of experimental groups. (A) Light micrograph of normal control rats showing normalrenal tubular epithelial cells in pancreatic islet (H & E, 40x), (B) HFD-STZ induced diabetic control rats showing the fatty degeneration of renal tubular epithelial cells (H & E, 40x), (C) MDCCCL1636 at 7.5 mg/kg/day resulted in the reversal of the fatty degeneration of renal tubular epithelial cells (H & E, 40x), (D) pioglitazone at 30 mg/kg/day showing no effect on the fatty degeneration of renal tubular epithelial cells (H & E, 40x).